Anisotropic Vortex Structure in $Y_1Ba_2Cu_3O_7$

G. J. Dolan,[a] F. Holtzberg, C. Feild, and T. R. Dinger
IBM Research Division, T. J. Watson Research Center, Yorktown Heights, New York 10598
(Received 6 March 1989)

We report Bitter-pattern observations of the vortices for flux trapped in crystals of the orthorhombic high-T_c superconductor $Y_1Ba_2Cu_3O_7$. For $\mathbf{B}\parallel\mathbf{c}$ axis, the slight distortion of the vortex lattice yields a penetration-depth anisotropy ranging from 1.11 to 1.15 for different crystals. For $\mathbf{B}\perp\mathbf{c}$, the case of strong anisotropy, we observe chains of oval vortices. When they are not aligned by defects, the chains appear to undulate rather than adopt a crystalline habit. From the vortex spacing we deduce an anisotropy of 5.5 ± 1.

PACS numbers: 74.70.Vy, 61.16.Di, 74.60.Ge

In a magnetic field a type-II superconductor enters a mixed state of normal-phase vortices in a superconducting matrix. The structure of the mixed state strongly influences magnetic and transport properties. In the new superconductors, the mixed state has basic similarities to those found in conventional materials but several unique properties are proven or suggested in experiment[1-7] or theory.[8-10] Bitter patterns[1-3] provide information on the vortices which is unusually direct in testing assumptions about the nature of the mixed state but have not so far been used to address the extraordinary anisotropy in many of the new superconductors. We have studied the effects of anisotropy for the important material $Y_1Ba_2Cu_3O_7$ and see striking contrasts with the well-known isotropic case. We also use the patterns to make measurements of the anisotropy in the superconducting penetration depth λ. We do this first for a low-anisotropy orientation, where such a measurement is difficult by other means, and then for the highest-anisotropy orientation, where macroscopic measurements have produced conflicting results.[6] The observations and measurements provide information important for the new field of high-T_c superconductivity but we believe they are also the first observations of their kind in any superconductor of such high anisotropy.

In an isotropic superconductor in weak fields (i.e., low vortex density), the vortex field and intervortex forces fall off from the vortex center essentially as $\exp(-r/\lambda)$. The repulsive vortex force results in a stable lattice, with the close-packed hexagonal lattice being favored.[11] In the anisotropic case it is usual to express the anisotropy in terms of an effective mass ratio for the carriers: $m_{i,j}=M_{i,j}/M_{\text{ave}}$.[10] As in Ref. 6, for vortices along one of the axes, we will consider the anisotropy in terms of a physical penetration depth $\lambda_{i,j}$, where the subscripts denote the axis along which the field lies and the direction of field decay. The terminology is sufficient for the special cases. The penetration-depth ratios we measure are simply the roots of corresponding mass ratios. One expects the vortex magnetic shape and any lattice to be distorted by the anisotropy in λ, as if the coordinate system were compressed in one direction. The latter can be seen by assuming that the form of the intervortex force remains unchanged and realizing that for any stable array the forces remain in balance even in the presence of anisotropy in the forces.

The Bitter-pattern technique "decorates" a sample with fine ferromagnetic particles to reveal the pattern of magnetic flux as it emerges from a sample surface.[1-3,12] The patterns depend on the field conditions and history as well as on the material properties. Our experiments reveal flux trapped as the sample is cooled in a constant field. The vortex positions are those attained as the vortices are "frozen" in place at some temperature where pinning prevents further vortex motion.[2] After decoration, the sample is warmed to room temperature to examine the pattern using scanning electron or optical microscopy. For the low-anisotropy case, images were digitized and digitally Fourier transformed to obtain measurements of anisotropy in the average vortex spacing. Careful attention was paid to avoid the introduction of systematic error in the measurements from distortions in the various imaging steps. The $Y_1Ba_2Cu_3O_7$ crystals were of a kind often studied.[1-6,13] Generally, they have smooth surfaces normal to the primary crystal axes so that these surfaces are candidates for the decoration experiments. Also, they have many "twins," crystal regions with the almost identical axes **a** and **b** interchanged. The twin boundaries are {110} planes parallel to the long crystal axis, **c**, and at very nearly 45° to **a** and **b**. The boundaries and the crystal faces provide means of determining crystal orientation but not the distinction between **a** and **b**.

$\mathbf{B}\parallel\mathbf{c}$, *small-anisotropy case.*—In twin-free regions, one observes good vortex lattices[2] whose distortion is accurately measured by taking the two-dimensional Fourier transform of the pattern. One expects at most a small anisotropy since the *b* crystal spacing exceeds the *a* spacing by only $\approx 1.8\%$. Anisotropies of, say, 50% would have been immediately apparent in the earlier work.[1-3] Figure 1 shows Fourier transforms at two fields for a sample decorated successively in fields of 40 and 80 G. This resulted in average trapped-flux magnitudes of $\bar{B}\approx 35$ and 65 G. The figure shows the summed trans-

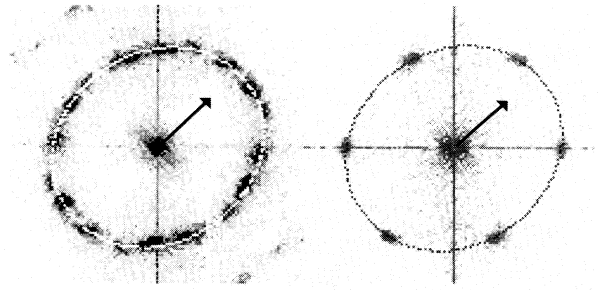

FIG. 1. Digital Fourier transform of the vortex patterns observed at two fields ($\bar{B}=35$ and 65 G) parallel to the **c** axis of a $Y_1Ba_2Cu_3O_7$ crystal. Transforms from a sampling of different areas are shown. Ellipsoids whose eccentricity corresponds to the λ anisotropy are superimposed. The scale should be considered arbitrary. The arrow indicates the **a** crystal axis.

FIG. 2. Isolated, oval vortices observed at a very low field oriented perpendicular to the **c** axis. The **c** axis is horizontal in this and the following figures. The marker is 1 μm.

forms for a sampling of different areas for both fields. This sampling was done to average over any distortions arising from gradients or stress in the vortex lattice. At the lower field, the averaging produces a "powder pattern" corresponding to the diffraction pattern of many small vortex-lattice crystallites. At the higher field a particular orientation dominates sufficiently strongly that an almost hexagonal pattern is obtained even after averaging. Ellipsoidal shapes were fitted to the transforms using the ellipse eccentricity, orientation, and minor axis as parameters. Fits of distorted hexagons using the same parameters produce a measurement of the same accuracy. The ellipses are oriented along the crystal **a** axis (arrow); the axis direction was determined by x-ray analysis. The eccentricity at both fields is $f^{-1}=1.15\pm0.02$. Of course, the x-space distortion is f rather than f^{-1}. The penetration-depth ratio is $f=\lambda_{c,b}/\lambda_{c,a}=1.15\pm0.02$. Measurements on four other crystals produced distortions as small as 1.11 ± 0.02. The variation is between crystals, not on a given crystal. The distinction between **a** and **b** was not made in these instances and it is only assumed that the direction of distortion remains the same. We conclude that there is an anisotropy of about 1.13 in $Y_1Ba_2Cu_3O_7$ but that variations of at least the range detected can be expected in different samples. For comparison, we mention peripheral, limited experiments. For a PbTl alloy (a traditional superconductor) we observed no anisotropy within our sensitivity ($<2\%$). For $Bi(SrCa)_2Cu_3O_7$ we observed a lattice anisotropy of 0.2 ± 0.2, so any anisotropy in this case is at the margin of our resolution.

B $\perp$ **c**, *high-anisotropy case.*—Here we will show direct images of the decoration patterns. The plane decorated is composed of twins, i.e., a combination of a-c and b-c planes. While we measured the small difference between **a** and **b** above, here we will assume they are essentially equal, focusing on the large difference associated with the long **c** axis. Experimentally, the situation is difficult because of the rarity of crystals with a large c dimension and, more fundamentally, because the larger vortex magnetic area results in much smaller driving fields for the magnetic particles. We obtained clearly resolved vortices only in very low fields and for only a few of about forty decorations. What we will call "chains" of vortices were resolved almost always, however.

At fields comparable to the Earth ambient we observed approximately uniform sprinklings of essentially isolated, oval-shaped vortices. Figure 2 shows a few such vortices. Their shape reflects the shorter penetration depth, $\lambda_{b,c}$, along the **c** direction compared to $\lambda_{b,a}$. One would infer from the vortex shape an anisotropy of from 2 to 4. However, general considerations regarding the image formation and detection convince us that the images produce only a lower bound on the anisotropy. An increase in field produced observable vortex interactions and some suggestion of order. Figure 3 shows this for a sample cooled in 4 G. Using the criteria of Ref. 1, one concludes that the ovals are singly quantized vortices of flux quantum $\Phi_0=hc/2e$. The vortices form horizontal chains often aligned with twin boundaries in the crystals. In these respects the patterns are similar to the more isotropic case.[1,2] The interaction with the twin boundaries cannot be so simple, however, since the boundaries intersect the surface at a 45° angle and all the vortices must pass through boundaries in the crystal bulk.

The anisotropy in λ is determined from the nearest-neighbor distance between vortices. Although there are many local disturbances from defects, the overall anisotropy in nearest-neighbor distance should reflect the anisotropy in λ. The distance between horizontal vortex chains in the vicinity of Fig. 3 is ≈ 6.7 μm while the average spacing within a stripe is 1.2 μm. Taking this ratio as the anisotropy and considering variations at oth-

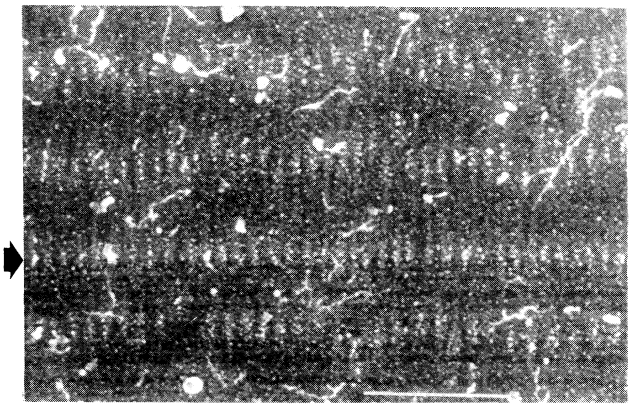

FIG. 3. Horizontal chains of oval vortices at a field 4 G perpendicular to the **c** axis. The arrow indicates the position of a twin boundary which aligns a vortex chain. The bright, irregular objects are irrelevant debris. The marker is 10 μm.

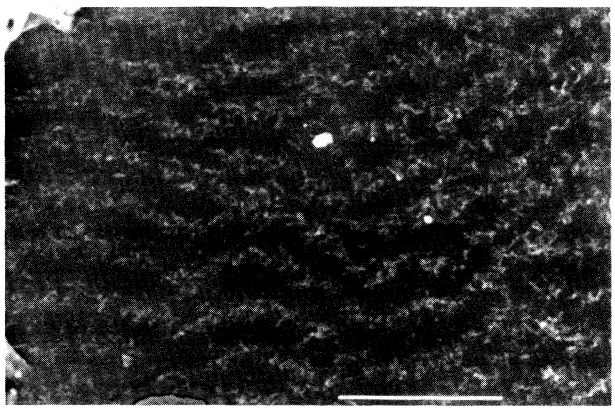

FIG. 4. Pattern observed at a field of 8 G perpendicular to **c**. Individual vortices are not resolved but the undulating chains are observable. The marker is 10 μm.

er regions on the sample, we obtain $f=\lambda_{a,b}/\lambda_{a,c} \approx \lambda_{b,a}/\lambda_{b,c}=5.5\pm 1$ for this sample. Only one other sample provided a comparably good measurement. The results agreed within the range of error. Most often, the linear chains of vortices discussed below were observed but vortices were not resolved within chains. Properly, the chain spacing varied as $\sqrt{B}$ and was consistent with a similar anisotropy in all the samples. The measurement corresponds to an effective mass ratio of 30 but with only 40% accuracy. The λ anisotropy result exceeds that of Krusin-Elbaum *et al.*[6] by about 2 and is in better agreement with some older results discussed by those authors.

In Fig. 3 the vortices align in horizontal chains of vortices with a tendency to anticorrelation between vortices in adjacent chains; i.e., a vortex in a chain aligns with a gap in the next chain. This is a characteristic of one of the orientations of the distorted hexagonal lattice discussed by Campbell and co-workers[10] and the observation might be regarded as the beginnings of a lattice of this orientation. However, in Fig. 3 the pattern is influenced by the presence of a twin domain boundary (arrow) which strongly aligns one chain. It is significant that the adjoining chains (no twin boundaries) begin a slight modulation in the vertical ($\perp$**c**) direction with a period of about eight (horizontal) vortex spacings. The chains of vortices seem to be an inherent feature of the patterns but oriented chains do not appear to be a stable configuration except when stabilized by a twin boundary or other sample feature.

In contrast to the nearly isotropic case (Fig. 1), increasing the field does not produce more ordered structures or aligned chains. Figure 4 shows a pattern obtained on a sample cooled in a field of 8 G. The chains, but not individual vortices, are resolved. This type of pattern was observed many times and at fields comparable to those studied in the almost isotropic case. Aside from their strong interaction with defects, the chains' primary characteristics are a tenacious continuity and their tendency to corrugation with a rough, characteristic period. The corrugations may indicate that the equilibrium lattice contains a superimposed lattice or superlattice or that there is an inherent instability in any fixed lattice. There is a general basis for the latter suspicion. For an anisotropy of $f=5.5$ in λ, Kogan and Campbell[10] predict a shear modulus anisotropy of $f^4 \approx 900$. In this situation, small displacements of a vortex (vertically in the figures) are so easy to produce that any lattice is subject to virtually any mechanism of distortion. Still, one is left with explaining the mechanism. Also, one must consider the effect of the twin boundaries for this case where the boundaries pass obliquely beneath the surfaces on which the vortices are imaged.

In conclusion, we have used the Bitter-pattern technique to measure the λ anisotropy in the new superconductor $Y_1Ba_2Cu_3O_7$ for the simplest cases. The values obtained have considerable uncertainty and apply strictly only to the few samples tested. On the other hand, the measurements are derived straightforwardly from the elemental magnetic vortex interaction and, as far as they go, should be considered reliable. A possible difficulty in the method is that the vortex positions are frozen in place at some unknown, high temperature. This is a problem only if there is a significant temperature dependence to the anisotropy. There is no basis for such an assumption.[6] We have also shown the first images of one of the novelties of this new superconductor, the oval vortex. These vortices do not appear to order in the most straightforward way, but show a tendency to form corrugated chains. This unusual vortex arrangement will influence macroscopic magnetic and transport properties and is a matter of some importance.

We gratefully acknowledged discussions with and assistance from R. Collins, J. R. Kirtley, R. Webb, J. J. Wainer, I. M. Fisher, W. Krakow, T. Shaw, A. Stein,

and especially V. G. Kogan and L. J. Campbell for their discussions and advice on the experiments; R. F. Boehme for his x-ray analysis of our lightly twinned crystal; and G. V. Chandrashekhar for supplying the $Bi(SrCa)_2Cu_3O_7$ crystal mentioned.

---

[a]Present address: Physics Department, University of Pennsylvania, Philadelphia, PA 19104.

[1]P. L. Gammel, D. J. Bishop, G. J. Dolan, J. R. Kwo, C. A. Murray, L. F. Schneemeyer, and J. V. Waszczak, Phys. Rev. Lett. **59**, 2592 (1987).

[2]G. J. Dolan, G. V. Chandrashekhar, T. R. Dinger, C. Feild, and F. Holtzberg, Phys. Rev. Lett. **62**, 827 (1989).

[3]L. Ya. Vinnikov, L. A. Gurevich, G. A. Emel'chenko, and Yu. A. Osip'yan, Pis'ma Zh. Eksp. Teor. Fiz. **47**, 109 (1988) [JETP Lett. **47**, 131 (1988)]; Yu. A. Osip'yan, V. B. Timofeev, and I. F. Schegolev, Physica (Amsterdam) **153C-155C**, 1133 (1988).

[4]K. A. Müller, M. Takashige, and J. G. Bednorz, Phys. Rev. Lett. **58**, 1143 (1987); T. K. Worthington, W. J. Gallagher, and T. R. Dinger, Phys. Rev. Lett. **59**, 1160 (1987); A. P. Malozemoff, T. K. Worthington, Y. Yeshurun, F. Holtzberg, and P. H. Kes, Phys. Rev. B **38**, 7203 (1988); Y. Yeshurun and A. P. Malozemoff, Phys. Rev. Lett. **60**, 2202 (1988); M. Tinkham, Phys. Rev. Lett. **61**, 1658 (1988).

[5]P. L. Gammel, L. F. Schneemeyer, J. V. Waszczak, and D. J. Bishop, Phys. Rev. Lett. **61**, 1666 (1988).

[6]L. Krusin-Elbaum, A. P. Malozemoff, Y. Yeshurun, D. C. Cronemeyer, and F. Holtzberg, Phys. Rev. B **39**, 2936 (1989); L. Krusin-Elbaum, R. L. Greene, F. Holtzberg, A. P. Malozemoff, and Y. Yeshurun, Phys. Rev. Lett. **62**, 217 (1989). These recent works discuss and cite earlier measurements of the λ anisotropy.

[7]D. E. Farrell, C. M. Williams, S. A. Wolf, N. P. Bansal, and V. G. Kogan, Phys. Rev. Lett. **61**, 2805 (1988).

[8]D. R. Nelson, Phys. Rev. Lett. **60**, 1973 (1988).

[9]M. P. A. Fisher (to be published).

[10]L. J. Campbell, M. M. Doria, and V. G. Kogan, Phys. Rev. B **38**, 2439 (1988); V. G. Kogan, and L. J. Campbell, Phys. Rev. Lett. **62**, 1552 (1989).

[11]Michael Tinkham, *Introduction to Superconductivity* (McGraw-Hill, New York, 1975).

[12]U. Essmann and H. Träuble, Phys. Lett. **24A**, 526 (1967); N. V. Sarma, Philos. Mag. **17**, 1233 (1968).

[13]D. L. Kaiser, F. Holtzberg, B. A. Scott, and T. R. McGuire, Appl. Phys. Lett. **51**, 1040 (1987); D. L. Kaiser, F. Holtzberg, M. F. Chisolm, and T. K. Worthington, J. Cryst. Growth **85**, 593 (1987).

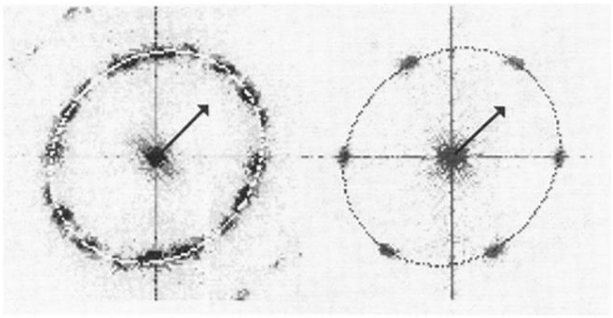

FIG. 1. Digital Fourier transform of the vortex patterns observed at two fields ($\bar{B}=35$ and 65 G) parallel to the **c** axis of a $Y_1Ba_2Cu_3O_7$ crystal. Transforms from a sampling of different areas are shown. Ellipsoids whose eccentricity corresponds to the λ anisotropy are superimposed. The scale should be considered arbitrary. The arrow indicates the **a** crystal axis.

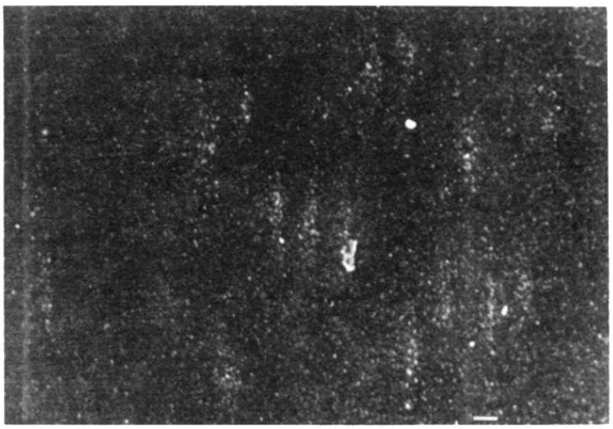

FIG. 2. Isolated, oval vortices observed at a very low field oriented perpendicular to the **c** axis. The **c** axis is horizontal in this and the following figures. The marker is 1 μm.

FIG. 3. Horizontal chains of oval vortices at a field 4 G perpendicular to the **c** axis. The arrow indicates the position of a twin boundary which aligns a vortex chain. The bright, irregular objects are irrelevant debris. The marker is 10 μm.

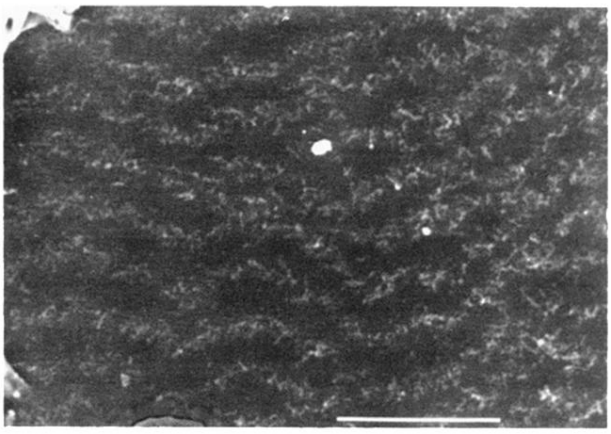

FIG. 4. Pattern observed at a field of 8 G perpendicular to **c**. Individual vortices are not resolved but the undulating chains are observable. The marker is 10 μm.